BULLETIN OF THE POLISH ACADEMY OF SCIENCES
TECHNICAL SCIENCES, Vol. 69(3), 2021, Article number: e137388
DOI: 10.24425/bpasts.2021.137388

Fluidized bed in gravitational shelf dryers: optimization calculation

Nadiia ARTYUKHOVA[1], Jan KRMELA[2*], Vladimíra KRMELOVÁ[3], Artem ARTYUKHOV[1], and Mária GAVENDOVÁ[3]

[1] Sumy State University, Oleg Balatskyi Academic and Research Institute of Finance, Economics and Management, Department of Marketing, Rymskogo-Korsakova st. 2, 40007, Sumy, Ukraine

[2] Alexander Dubček University of Trenčín, Faculty of Industrial Technologies in Púchov, Department of Numerical Methods and Computational Modeling, Ivana Krasku 491/30, 020 01 Púchov, Slovakia

[3] Alexander Dubček University of Trenčín, Faculty of Industrial Technologies in Púchov, Department of Material Technologies and Environment, Ivana Krasku 491/30, 020 01 Púchov, Slovakia

Abstract. The article deals with studying the hydrodynamic characteristics of the fluidized bed in gravitation shelf dryers. The algorithm to calculate hydrodynamic characteristics of the fluidized bed in the dryer's workspace is described. Every block of the algorithm has a primary hydrodynamic characteristics theoretical model of calculation. Principles of disperse phase motion in various areas in the gravitation shelf dryer are established. The software realization of the author's mathematic model to calculate disperse phase motion trajectory in a free and constrained regime, disperse phase residence time in the dryers' workspace, polydisperse systems classification is proposed in the study. Calculations of disperse phase motion hydrodynamic characteristics using the software product ANSYS CFX, based on the author's mathematic model, are presented in the article. The software product enables automating calculation simultaneously by several optimization criteria and visualizing calculation results in the form of 3D images. The disperse phase flow velocity fields are obtained; principles of a wide fraction of the disperse phase distribution in the workspace of the shelf dryer are fixed. The way to define disperse phase residence time91 in the workspace of the shelf dryer in free (without consideration of cooperation with other particles and dryer's elements) and con-strained motion regimes is proposed in the research. The calculation results make a base for the optimal choice of the gravitation shelf dryer working chamber sizes.

Key words: multistage gravitational shelf dryer; fluidized bed; hydrodynamics; motion trajectory; simulation of engineering calculation.

1. Introduction

Implementing a fluidized bed in heat-mass transfer processes has become widespread due to the undoubted advantages of such a hydrodynamic system [1–3]. At the same time, there are often difficulties in devices with a fluidized bed providing the required hydrodynamic regime. In this regime, the dispersed phase is predicted to spend the estimated time needed to complete the process in the device. In this case, a significant advantage of devices with a fluidized bed is the ability to control the residence time of the dispersed phase in the device's workspace [4]. Despite the variety of granulation and drying devices (an overview of methods for obtaining granulated dispersed materials is given, for example, in [5–12]), multistage devices with vertical sectioning of the working space did not receive a wide distribution for drying. The effectiveness of such devices has been proven by the example of various classifiers and granular devices [13–18], which confirms the relevance of their further implementation in the drying technology. The authors of this work attempted a theoretical description [19], experimental studies of the fluidized bed configuration [20], and the conditions for the implementation of heat-mass transfer processes [21] in other devices with the directed motion of the dispersed phase – vortex granulators [22].

The device and principle of a multistage gravitational shelf dryer's operation can be found in the following studies [23].

The article aims to form an algorithm for calculating the hydrodynamic parameters of the flow in devices with inclined shelves to implement heat treatment and dehydration processes. The research results will complement the general algorithm for the engineering calculation of shelf units, which authors begin to study in the research [24].

The authors use the hypothesis of the possibility to control the motion trajectory and the residence time of the dispersed phase in the dryer's workspace thanks to its directed transfer mechanisms (as shown in work [25]). The joint solution of the fundamental equations of flow motion hydrodynamics, the kinetics of change of the temperature-humidity features in the interacting flows, and the growth rates of granules will allow inventing a rational design of the workspace, heat transfer agent's optimum flow rate and its temperature-humidity features in a shelf dryer. The calculation is carried out by the optimization criterion of the "minimum" hydrodynamic "residence time of the dispersed phase in the workspace of the device". "Hydrodynamic" time should be equal to "kinetic" time – the period during which the temperature and moisture content features of the dispersed phase should acquire a normative value. This paper presents an algorithm for calculating the "hydrodynamic" residence time of dispersed particles in a shelf

*e-mail: jan.krmela@tnuni.sk

Manuscript submitted 2020-10-15, revised 2021-03-31, initially accepted for publication 2021-04-21, published in June 2021

dryer's working space. At the same time, the drying operating temperature was maintained in the dryer, which, for example, for granules of porous ammonium nitrate was 105–110°C. This algorithm is a continuation of work [26] on the study of convective dryers.

2. Physical model of the flow motion hydrodynamics and the drying process of dispersed materials in a shelf dryer

2.1. General statements. There are multiphase flows of different nature. Their survey is observed, for example, in [27–29] for various processes. The following types of multiphase flows should be distinguished. In the first case, the considered volume is filled with the substance of one phase. The sub-stance of another phase occurs in the form of discrete particles (solid phase) or bubbles (gaseous phase) where the volume rate of the substance of the other phase is low (up to 10% of the total volume). In the second case, the considered volume is partially filled with liquid and partly with gas, which does not mix, and the free surface separates them from each other. In the most challenging case, substances of different phases can mix (dissolve/stand out from solution), and the volume rate of the substance of another phase is significant (over 10% of the total volume). Various approaches are used to model these multiphase flows.

In many cases, it is possible to use the dispersed particles model, the mixing model, and the multiphase Euler model, to simulate flows in which substances of different phases can mix and do not form a free surface. Additional criteria for choosing a model include [29].

Ratio β of substance mass of the dispersed phase (df) to the substantial mass of the carrier phase (cf) [30]:

$$\beta = \psi \frac{V_{df}}{V_{cf}}, \tag{1}$$

where V_{df} and V_{cf} are volumes of the dispersed and carrier phases, ψ is the ratio of the dispersed and carrier phases density, $\psi = \rho_{df}/\rho_{cf}$; ρ_{df} – dispersed phase density; ρ_{cf} – carrier phase density; this ratio can be over 1000 for solids in a gas flow, about 1 for solids in a liquid flow, and less than 0.001 for gas particles in a liquid flow [30].

At a low β ratio, dispersed particles practically do not affect the carrier phase flow, and any of the listed models can be used [30]. At very remarkably values of β, dispersed particles strongly affect the carrier phase flow, and only the multiphase Euler model should be used for the proper simulation of the flow. With average β values, one needs to calculate the Stokes number to select a suitable model, as described below.

Stokes number St [31]:

$$\mathrm{St} = \frac{\tau_{df}}{\tau_{cf}}, \tag{2}$$

where τ_{df} is the time describing the motion of particles, $\tau_{df} = (\rho_{df} d^2)/(18\mu_{cf})$, d is the particle diameter, μ_{cf} is the viscosity of the carrier phase, $\tau_{cf} = l_{cf}/u_{cf}$ is the time describing the carrier phase flow, l_{cf} is the peculiar length, u_{cf} is the peculiar velocity.

If $St \ll 1.0$, the dispersed phase particles almost do not deviate from the streamlines of the carrier phase, and any flow model can be used (as a rule, the mixing model is the least resource-intensive) [32]. If $\mathrm{St} > 1.0$, the trajectory of the dispersed phase particles completely does not coincide with the carrier phase streamlines, and the mixing model is unsuitable in this case: either the dispersed particles model or the multiphase Euler model must be used [32].

In the case under consideration, the dispersed phase motion trajectory applies to the dispersed particle model. The substance forming the main phase is assumed to be a continuous space, and its flow is modelled (depending on the flow turbulence degree) by the Navier–Stokes or Reynolds equations and the flow continuity. The substance in the flow in the form of discrete particles does not form a continuous medium. Individual particles interact with the flow of the main phase and with each other discreetly. The Lagrange approach is used to model the motion of the particles of the dispersed phase. It means that the separate particles of the dispersed phase influenced by forces from the side of the main phase flow are controlled.

It should be noted that there is a constrained motion of particles (discrete particles, a solid phase, occupies a volume greater than 10% of the total space in the device) in the industrial model of a shelf dryer. In this case, the calculation model should be supplemented with a block that allows defining how the particles' residence time changes (increases) in the dryer if the volume of particles increases more than 10% [30].

The fraction composition of particles (distribution by size), the motion of which is modelled in this work, is shown in Fig. 1.

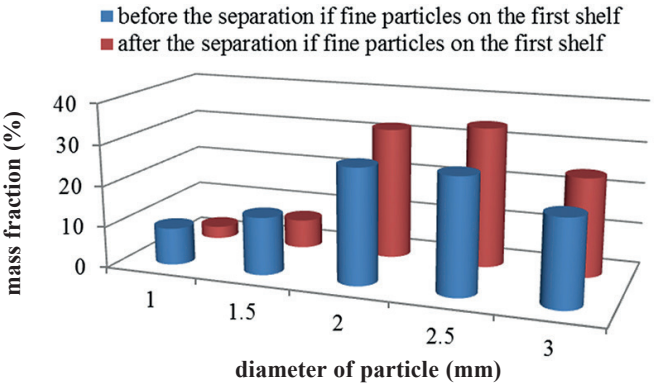

Fig. 1. Fraction composition of particles

The first (upper) shelf of the dryer serves as a separator for fine particles. Therefore, there is a change in the fractional composition towards increasing the commercial fraction's relative content.

2.2. Modelling of the gas flow motion. The previous experimental studies [33] demonstrate that the gas flow in the shelf dryer is turbulent. Direct modelling of the turbulent flows by

calculating the Navier – Stokes equations written for instantaneous velocities is complicated. Besides, not instantaneous, but time-averaged velocity values attract attention. For the analysis of turbulent flows, the Reynolds equation and the continuity of the flow are used [2, 26]:

$$\frac{\partial}{\partial \tau}\left(\rho_{cf}\overline{u_{cfi}}\right)+\frac{\partial}{\partial x_j}\left(\rho_{cf}\overline{u_{cfi}u_{cfj}}\right)+\frac{\partial}{\partial x_j}\left(\rho_{cf}\overline{u'_{cfi}u'_{cfj}}\right)$$
$$=-\frac{\partial p}{\partial x_i}+\frac{\partial}{\partial x_j}\left[\mu_{cf}\left(\frac{\partial \overline{u_{cfi}}}{\partial x_j}+\frac{\partial \overline{u_{cfj}}}{\partial x_i}\right)\right]+f_i\,, \tag{3}$$

$$\frac{\partial \rho_{cf}}{\partial \tau}+\frac{\partial}{\partial x_j}\left(\rho_{cf}u_{cfj}\right)=0, \tag{4}$$

where $\overline{u_{cf1}}$, $\overline{u_{cf2}}$, $\overline{u_{cf3}}$ – time-averaged velocities of carrier phase, $\overline{u'_{cf1}}$, $\overline{u'_{cf2}}$, $\overline{u'_{cf3}}$ – pulsation component of velocities of carrier phase.

In equations (3) and (4), the simplified equations are used, i, $j=1\ldots3$, the summing up to over the same indices are assumed, x_1, x_2, x_3 – coordinate axes, τ – time. The f_i term expresses the action of mass forces.

In this system of 4 equations, the independent sought parameters are three velocity components u_{cf1}, u_{cf2}, u_{cf3} and pressure p. The density ρ_{cf} of the gas, at velocities up to about 0.3 of the Mach number, can be assumed to be constant.

As the boundary conditions, the adhesion condition is set on all solid walls (the velocity is zero), the distribution of all velocity components in the inlet section, and the first derivatives (in the direction of flow) of the velocity components in the outlet section are equal to zero. Besides, the direct interest is the distribution of the velocity along the length of the device in space above the shelf, where the motion of dispersed particles occurs.

The range of existence of a fluidized bed in a shelf device is limited by such two boundary conditions or two critical gas flow (carrier phase) velocities: (*i*) the first critical velocity or the velocity of the start of fluidization; (*ii*) the second critical velocity or the velocity of the start of ablation. The values of these velocities depend on the size (diameter) of the dispersed phase, the flow rate of the carrier phase, and the velocity in the overhead space of the device (depends on the value of the free section of the shelf, its tilt angle, length, etc.).

2.3. Modelling of the particle motion in free motion mode. Let us assume that the dispersed phase particles have a spherical shape. The forces influencing this particle are caused by the difference between the particle velocity and the flow velocity in the main phase and the displacement of the main phase by this particle. The equation regarding the motion of such a spherical particle is as follows [28]:

$$m_{df}\frac{du_{df}}{d\tau}=3\pi\mu_{df}dC_{cor}\left(u_{cf}-u_{df}\right)+\frac{\pi d^3\rho_{cf}}{6}\frac{du_{cf}}{d\tau}$$
$$+\frac{\pi d^3\rho_{cf}}{12}\left(\frac{du_{cf}}{d\tau}-\frac{du_{df}}{d\tau}\right)+F_e\,, \tag{5}$$

where m_{df} – mass of the particle, d – diameter of the particle, u_{df}, u_{cf} – velocity; ρ_{df}, ρ_{cf} – density; μ_{df} – dynamic viscosity of the substance in the main phase, C_{cor} – its viscous resistance coefficient; F_e – an external force which is directly acting on a particle (for example, gravity, aerodynamic drag, centrifugal force etc.); index *df* refers to the dispersed phase, index *cf* refers to the carrier phase.

According to Stokes's law, the first term on the right-hand side of equation (5) expresses the deceleration of the particle as a result of viscous friction against the flow of the main phase. The second term is the force applied to the particle due to the pressure drop in the main phase surrounding the particle caused by the main phase flow's acceleration. The third term is the force required to accelerate the main phase's weight in the volume displaced by the particle.

The detailed description of this model is described in work [27] in applying three-phase vortex separators.

2.4. Modelling of particle motion in the constrained motion mode. Let us consider the motion of a particle in the inter-shelf space. At air velocity $u_{cf}>u_{cr1}$ in the shelf space (u_{cr1} – the first critical velocity or the velocity of the start of fluidization), it will be in a weighted state until it reaches $u_{cf}=u_{cr2}$, causing the ablation (u_{cr2} – the second critical velocity or the velocity of the start of ablation). If the air velocity is $u_{cf}<u_{cr2}$, then this difference of velocities $\Delta u_{cf}=u_{cr2}-u_{cf}$ will make the particle to move from top to bottom. If $u_{cf}<u_{cr1}$, the particle will move in the gravitational falling layer mode with a sharp decrease in the residence time on the shelf. Given that the gas flow transmits up to 95% of the momentum of the dispersed material, we suppose that the difference in particle velocities Δu_{df} will be approximately equal to the difference of velocities Δu_{cf} $\left(u_{df}\approx u_{cf};\ \Delta u_{df}=u_{cr2}-u_{df}\right)$.

The time of the particle motion along the shelf with the tilt angle $\gamma=90°$, and the length L_s on the i-th stage of the shelf device will be equal to:

$$\tau_i=\frac{L_s}{\Delta u_{df}}\approx\frac{L_s}{\Delta u_{cf}}\,. \tag{6}$$

In the case when the tilt angle of the shelf is small (in practice within 10–35°), the velocity Δu_{df} that describes the motion of the particle from top to bottom, will have one roll down component $\Delta u_{df}\cdot\sin\gamma$, because the normal reaction of the shelf will compensate the normal force of particle pressure on the shelf and, accordingly, standard acceleration components and velocities $\Delta u_{df}\cdot\cos\gamma$.

Thus, the motion time of the particle τ_i along the shelf on the i-th stage is calculated by the equation:

$$\tau_i=\frac{L_s}{\Delta u_{df}\sin\gamma}\,, \tag{7}$$

which is simplified with $\gamma=90°$ to the previous expression (6).

The ratio of the particle's motion time along the shelf is inversely proportional to the sines of the tilt angle γ of the shelf:

$$\frac{\tau_1}{\tau_2} = \frac{\sin\gamma_2}{\sin\gamma_1}. \tag{8}$$

According to these considerations, it is possible to define the possible constructive influence on the residence time of the particle in the inter-shelf space and the regulation of the drying process. The residence time of the dispersed particle (drying time) at this stage is increased by reducing the tilt angle of the shelf.

Formula (7) allows defining the residence time of a particle on the shelf that moves independently of other particles, i.e. its free motion is considered. Such free motion is observed only at small volumetric contents of the dispersed phase in a two-phase system when there is such a distance between the particles where collisions or mutual influence of the particles are absent. If $\delta \geq 0.1$ (constrained particle motion), there are some changes in the system: the distances between the particles' surfaces or the size of the passages between the particles become smaller than their diameter, and the particle cannot slip freely between the other two particles [34]. It is necessary to consider the collision effect of particles with each other. Besides, the collision of particles in a two-phase system can also occur when the dispersed phase consists of polydisperse particles or particles with different densities.

It is possible to consider the limited particle motion phenomenon and the interphase interaction force when introducing the constraint coefficient of the particle χ.

Various formulas are obtained to identify the particles constraint coefficient based on different dispersed phase particle location schemes. In particular, the following formula considers the scheme with random free filling [35]:

$$\chi = (1-\delta)^{-n}, \tag{9}$$

where δ – coefficient of constrained particle motion that takes into account the type of filling material; $\delta = 0.6$ (the case of random free filling [34]); n – exponent that takes into account the constraint of the material flow; $n = 3$–5 (accepted as preliminary data and should be specified by the experimental studies and computer modelling).

Thus, expression (7) will be as follows:

$$\tau_i = \frac{L_{sh} \cdot \chi}{\Delta u_{cf} \cdot \sin\gamma}. \tag{10}$$

3. Results and discussions

Two blocks present the results from hydrodynamic indices calculations in the shelf dryer: the gas flow velocity over the dryer's shelf (the model in Section 2.2) and the residence time of particles in the device in constrained motion (combined model from Section 2.3 and 2.4).

3.1. The gas flow motion. Let us consider the dependence of the ascending velocities profile on the structural features of the inter-shelf space, namely, the length of the shelves, the degree of their perforation and the installation angle γ. The ascending velocities profile will have a peculiar peak in the inter-shelf space with no perforation (Fig. 2a).

In the presence of perforation, the peak decreases according to the increase in the drying agent's flow rate through the sectioning shelves holes (Fig. 2b). Optimization of the ascending velocity profile can be achieved not only by changing the outloading gap and the tilt angle of the shelves but also by varying the perforation degree along the shelves (Fig. 2c).

When establishing shelf contacts with different outloading gap, the epure of the gas flow velocity distribution has the following features:

- the distribution of the gas flow velocity has a descending nature from the wall of the device to the end of the shelf contact. It is caused by the length difference of the pressure under the shelf contact and above it;
- when reducing the ratio of the current length to the length of the shelf X/L, starting from the middle of the shelf contact, there is an intense decrease in the gas flow velocity caused by the creation of swirls in the outloading gap. Reducing the outloading gap size leads to an increase in the intensity of swirls at the end of the shelf contact, which disrupts the ascending motion of the gas flow;
- the minimum velocity value of the gas flow at the shelf contact is greater, the smaller the outloading gap value is.

The results analysis regarding the gas flow velocity distribution at different stages of the dryer depending on their height with the same design of each stage showed that:

- the distribution of the gas flow velocity becomes more uniform with the increasing value of the outloading gap;
- the epure of the gas flow velocity for shelf contact of one structure quantitatively changes its profile. The gas flow redistribution causes it in the dryer's cross-section in height, and with the height, it becomes more uniformed.

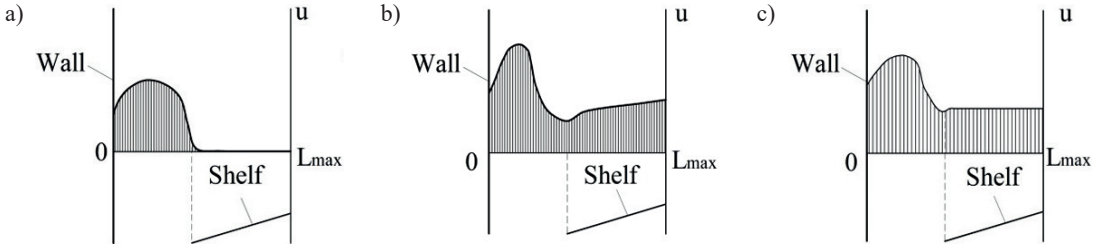

Fig. 2. Gas flow velocity profiles: a) non-perforated shelf; b) perforated shelf with constant length perforation; c) perforated shelf with variable length perforation

When installing shelf contact with different values of the free cross-section (the free cross-section increase) in the dryer, the following situation is observed:

- the level of the gas flow motion velocity is partially levelled on a shelf contact;
- there is a decrease in the peak velocity of the gas flow in the outloading gap;
- the epure of the gas flow velocity in the transition from the shelf contact to the outloading gap has a smoother character.

Reduction of the shelf contact angle at a constant gap X/L puts its features in the epure of the gas flow velocity distribution:

- there is a decrease in the peak velocity of the gas flow on the shelf, the epure is levelled;
- the peak velocity of the gas flow decreases in the outloading gap;
- the zone of the gas flow maximum velocity in the outloading gap is expanded with the alignment of the epure.

The epure of the gas flow velocity distribution with increasing consumption has the same qualitative law but is characterized by the following distinctive features:

- smoothing of the peak in the middle of the shelf contact;
- levelling of the velocity along the length of the shelf contact;
- the peak velocity of the gas flow in the outloading gap is more expressed.

Epures of the gas flow velocity distribution enable to define the gravitational motion zones of the dispersed material, its soaring in the device, separation, and possible ablation. It is necessary to investigate the basic modes of the dispersed material motion to describe the hydrodynamics of the dispersed material motion, identify its motion trajectory and residence time in the dryer and the impact on these parameters of the shelf contact construction and gas flow rate.

3.2. The dispersed material motion. Analysis of the previous studies in the two-phase flows modelling field, which consist of gas as a dispersion phase and dispersed particles, shows that one of the most promising ways to calculate the motion of particles is the so-called trajectory method [36–38]. The authors [39, 40] conclude that in modelling, the constrained motion of particles with large (0.5–5 mm) diameter can be based on the Lagrangian model of force analysis of particle motion using differential equations of motion which have already been used to describe hydrodynamic conditions of dispersion phases in the workspace of the shelf device. At the same time, for the case of granules motion in the workspace of the device, the application of the trajectory method is complicated by the following:

- polydispersity of the system;
- constrained motion of granules in the shelf device.

Thus, the trajectory method with highly accurate results can be used only if there is software that allows one to export a theoretical model of the single-particle motion and consider the degree of flow constraint.

In this work, the software product Ansys Fluent is used to export the original mathematical model, to calculate the granules trajectories and the distribution law of the polydisperse system in the workspace of the shelf device, taking into account the concentration of the dispersed phase (the flow constraint).

Visualization of the results of modelling the motion of the polydisperse system is shown in Fig. 3 (relative content of the dispersed phase in the workspace is $\psi = 0.2$) with places for supply hot air and input of material for drying.

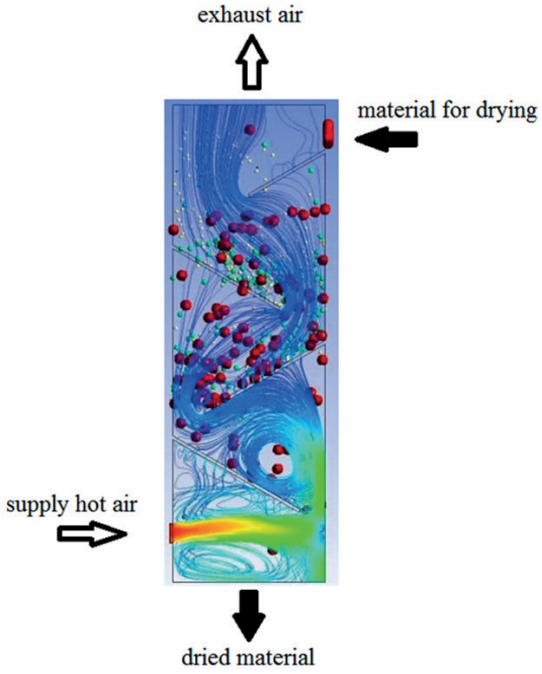

Fig. 3. Visualization of results of the polydisperse system constrained motion modelling in the shelf device

The methodology for carrying out this stage in the research allows inserting the calculated number of granules of a specific size as initial data (analog of the polydisperse system's fractional composition) and the total number of granules (analog of the degree of dispersed flow compression). With the help of this technique, it becomes possible to define the dispersed phase trajectories and refine the empirical constraint coefficient m to calculate the constrained motion time.

Figures 4–6 show data for calculating the residence time of dispersed material on the shelf in free and constrained mode. An example of comparing data for determining the residence time of dispersed material in the constrained mode according to the theoretical model is experimental and computer modelling data. In these figures, the shelf length – without taking into account the angle of inclination.

Data from Fig. 6 show that the results of computer modelling give a higher value of the residence time of the dispersed phase on the shelf in the device. It is explained by the inhibition of particles not only due to the action of neighbouring particles but also due to the creation of a vortex gas flow zone at the end of the shelf.

Based on the experimental research data analysis and computer modelling results, the value of the exponent m in formula

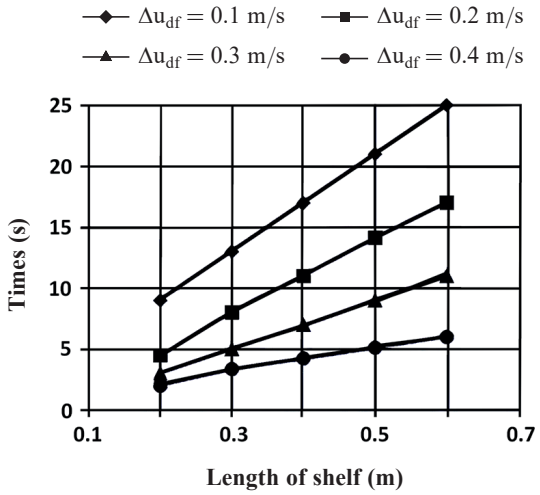

Fig. 4. Residence time of the particle on the shelf (free motion): $d_p = 2$ mm; $\psi = 0{,}25$, $\gamma = \gamma_0 + (11–13)°$

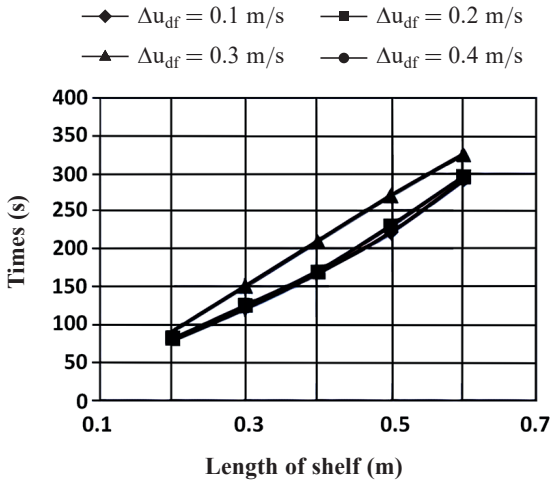

Fig. 5. Residence time of the particle on the shelf (constrained motion): $d_p = 2$ mm; $\psi = 0{,}25$, $\gamma = \gamma_0 + (11–13)°$, $\delta = 0.6$

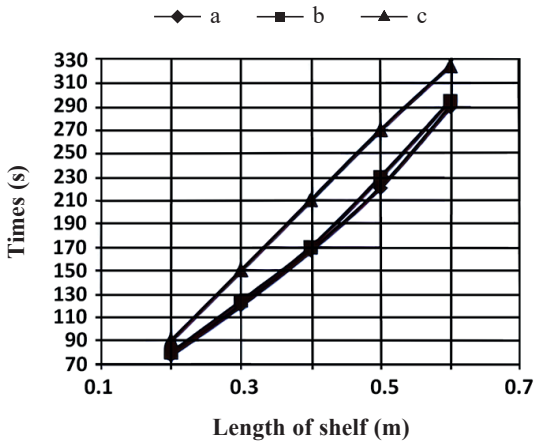

Fig. 6. Residence time of the particle on the shelf (constrained motion): $d_p = 2$ mm; $\psi = 0{,}25$, $\gamma = \gamma_0 + (11–13)°$, $\delta = 0.6$, $\Delta u_f = 0.2$ m/s; a – data from the theoretical calculation; b – data of the experimental studies (in the frame of this work); c – data of the computer modelling

(9) was refined. As can be seen from the graph shown in Fig. 5, the experimental range of the exponent differs little from the theoretical ones. However, in this work, it is recommended to use the indicator m, which is obtained from computer modelling, considering the peculiarities of the hydrodynamic picture at the end of the shelf. A narrower value of $n = 5.4–5.7$ is proposed.

Data from Fig. 6 show that the results of computer modelling give a higher value of the residence time of the dispersed phase on the shelf in the device. It is explained by the inhibition of particles not only due to the action of neighbouring particles but also due to the creation of a vortex gas flow zone at the end of the shelf.

Based on the experimental research data analysis and computer modelling results, the value of the exponent m in formula (9) was refined. As can be seen from the graph shown in Fig. 5, the experimental range of the exponent differs little from the theoretical ones. However, in this work, it is recommended to use the indicator m, which is obtained from computer modelling, considering the peculiarities of the hydrodynamic picture at the end of the shelf. A narrower value of $n = 5.4–5.7$ is proposed.

4. Conclusions

The research results in creating the software "Multistage fluidizer©" [41], which calculates the residence time of the material on the dryer's shelf, depending on its construction and features of the gas flow. The interface of the software and the results of some calculations are shown in Fig. 7. For the first time, this software was presented by the authors in work [26]. In this article, the software has been improved in terms of calculating the residence time of particles in a shelf unit in a constrained mode. The values of the coefficients given in the program are taken based on the literature data [2, 24].

The software makes it possible to predict the change in the residence time of dispersed material at the gravity shelf dryer stage and to obtain data on the optimal technical and economic indices of the device in terms of material flow rate for production and energy for creating a fluidized bed of a given configuration.

Also, it is planned to use the neural network [42, 43] for optimization of this calculation for further research:

- moisture of the material *i*-stage of the dryer *x* (kg of water/kg of material);
- moisture of the drying agent in *i*-stage of the dryer *b* (kg of water/kg of material)

Acknowledgements. The authors thank researchers at the Department of Marketing, Sumy State University and Department of Numerical Methods and Computational Modelling, Alexander Dubček University of Trenčín, for their valuable comments during the article preparation.

This research work had been supported by the Ministry of Science and Education of Ukraine under the project No. 0120U100476 "Technological bases of multistage con-

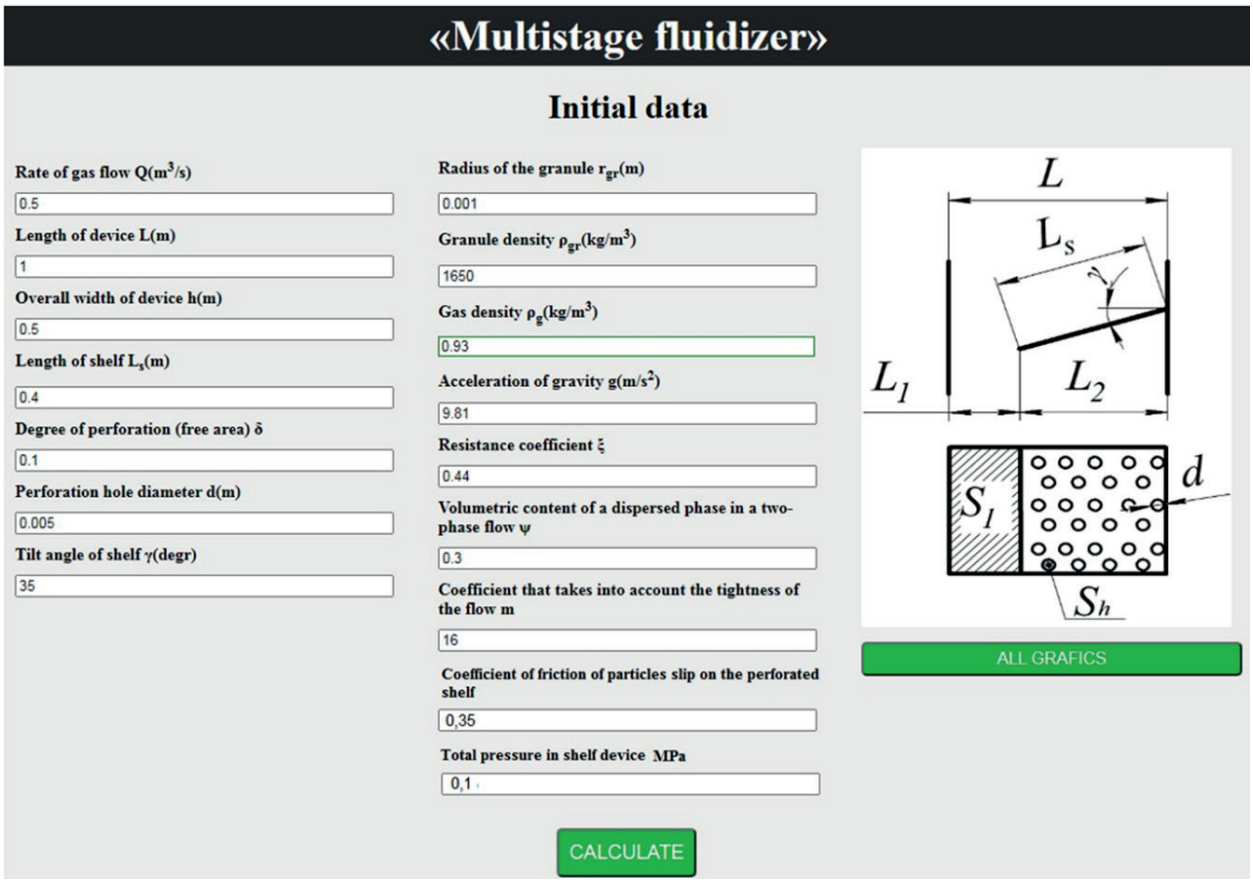

Fig. 7. Software "Multistage fluidizer" ©: the main window

vective drying in small-sized devices with utilization and heat recovery units" and the Cultural and Educational Grant Agency of the Slovak Republic (KEGA), project No. KEGA 002TnUAD-4/2019 "The influence of temperature and other parameters on the tensile properties of polymer composites and polymers under the uniaxial and biaxial cyclic loading" and the project "Advancement and support of R&D for "Centre for diagnostics and quality testing of materials" in the domains of the RIS3 SK specialization", ITMS2014: 313011W442.

Nomenclature

Variable

C_{cor} – viscous resistance coefficient of the dispersed phase;
d – diameter of the particle, m;
F_e – external forces, N;
fi – mass forces, N;
l – peculiar length, m;
L – length, m;
m – mass, kg;
n – exponent that takes into account the constraint of the material flow;
p – pressure, MPa;
u – velocity (general), m/s
$\bar{u}$ – time-averaged velocity, m/s
$\overline{u'}$ – pulsation component of velocity, m/s
u_{cr1} – first critical velocity or the velocity of the start of fluidization, m/s;
u_{cr2} – second critical velocity or the velocity of the start of ablation, m/s;
Δu – difference of velocities, m/s;
V – volume, m^3;
x – coordinate axis;
β – ratio of substance mass of the dispersed phase to the substance mass of the carrier phase;
γ – tilt angle of the shelf, degree;
δ – coefficient of constrained particle motion that takes into account the type of filling material;
ρ – density, kg/m^3
τ – time, s;
ψ – ratio of the dispersed and carrier phases density;
μ – dynamic viscosity, Pa·s;
χ – constraint coefficient of the particle.

Index

df – dispersed phase;
cf – carrier phase;
s – shelf.

Similarity criteria

St – Stokes number.

References

[1] M. Kwauk, *Fluidization: Idealized and bubbleless*, *with application*, Science Press, Beijing, 1992.

[2] D. Gidaspow, *Multiphase flow and fluidization: continuum and kinetic theory descriptions with applications*, Academic Press, San Diego, 1994.

[3] W.-C. Yang, *Handbook of fluidizfition and fluid-particle systems*, Marcel Dekker, New York, 2003.

[4] L.G. Gibilaro, *Fluidization-dynamics. The formulation and applications of a predictive theory for the fluidized state*, Butterworth-Heinemann, Woburn, 2001.

[5] P. Muralidhar, E. Bhargav, and C. Sowmya, "Novel techniques of granulation: a review", *Int. Res. J. Pharm*. 7(10), 8–13 (2016).

[6] H. Stahl, "Comparing Different Granulation Techniques", *Pharm. Technol. Eur.* 16(11), 23–33 (2004).

[7] D. Parikh, *Handbook of Pharmaceutical Granulation Technology*, Informa Healthcare, 2009.

[8] H. Stahl, *Comparing Granulation Method*, Hürth: GEA Pharma Systems, 2010.

[9] H.K. Solanki, T. Basuri, J.H. Thakkar, and C.A. Patel, "Recent advances in granulation technology" *Int. J. Pharm. Sci. Rev. Res.* 5(3), 48–54 (2010).

[10] S. Srinivasan, "Granulation techniques and technologies: recent progresses", *Bioimpacts* 5(1), 55–63 (2015).

[11] M.A. Saikh, "A technical note on granulation technology: a way to optimize granules", *Int. J. Pharm. Sci. Rev. Res.* 4, 55–67 (2013).

[12] P. Patel, D. Telange, and N. Sharma, "Comparison of Different Granulation Techniques for Lactose Monohydrate", *Int. J. Pharm. Sci. Drug. Res.* 3, 222–225 (2011).

[13] V.A. Kirsanov and M.V. Kirsanov, Effect of Structural Parameters of Cascade Elements on Effectiveness of Pneumatic Classification", *Chem. Pet. Eng.* 49, 707–711 (2014).

[14] V.A. Kirsanov and M.V. Kirsanov, "Hydrodynamic Characteristics of Classification Process in Pneumatic Classifier with Continuous Shelves", *Chem. Pet. Eng.* 54, 71–74 (2018).

[15] M. Yukhymenko, R. Ostroha, A. Lytvynenko, Y. Mikhajlovskiy, and J. Bocko, "Cooling Process Intensification for Granular Mineral Fertilizers in a Multistage Fluidized Bed Device", *Lecture Notes in Mechanical Engineering*, pp. 249–257, Springer, Cham, 2020.

[16] M. Yukhymenko and A. Lytvynenko, "Pneumatic Classification Of The Granular Materials In The "Rhombic" Apparatus", *J. Manuf. Ind. Eng.* 1–2, 1–3 (2014).

[17] E. Barsky and M. Barsky, "Master curve of separation processes", *Phys. Sep. Sci. Eng.* 13(1), 1–13 (2004).

[18] E. Barsky and M. Barsky. *Cascade Separation of Powders*, Cambridge Int Science Publishing, 2006.

[19] A.E. Artyukhov, V.K. Obodiak, P.G. Boiko, and P.C. Rossi, "Computer modeling of hydrodynamic and heat-mass transfer processes in the vortex type granulation devices", in *CEUR Workshop Proceedings*, 2017, 1844, pp. 33–47.

[20] A.E. Artyukhov and N.A. Artyukhova, "Utilization of dust and ammonia from exhaust gases: new solutions for dryers with different types of fluidized bed", *J. Environ. Health Sci. Eng.* 16(2), 193–204 (2018).

[21] A. Artyukhov, N.Artyukhova, A. Ivaniia, and R. Galenin, "Progressive equipment for generation of the porous ammonium nitrate with 3D nanostructure", *Proceedings of the 2017 IEEE 7th International Conference on Nanomaterials: Applications and Properties*, NAP 2017, 2017, p. 03NE06.

[22] A. Artyukhov, N. Artyukhova, J. Krmela, and V. Krmelova, "Complex designing of granulation units with application of computer and software modeling: Case "Vortex granulator". *IOP Conf. Ser.: Mater. Sci. Eng.* 776(1), 012016 (2020).

[23] N.A. Artyukhova, "Multistage finish drying of the N_4HNO_3 porous granules as a factor for nanoporous structure quality improvement", *J. Nano- Electron. Phys.* 10 (3), 03030-1-03030-5 (2018).

[24] A.E. Artyukhov, N.O. Artyukhova, and A.V. Ivaniia, "Creation of software for constructive calculation of devices with active hydrodynamics", in *Proceedings of the 14th International Conference on Advanced Trends in Radioelectronics*, *Telecommunications and Computer Engineering (TCSET 2018)*, 2018, pp. 139–142.

[25] A.E. Artyukhov, N.A. Artyukhova, A.V. Ivaniia, and J. Gabrusenoks, "Multilayer modified NH_4NO_3 granules with 3D nanoporous structure: effect of the heat treatment regime on the structure of macro- and mezopores", in *Proc IEEE International Young Scientists Forum on Applied Physics and Engineering (YSF-2017)*, 2017, pp. 315–318.

[26] A. Artyukhov, N. Artyukhova, R. Ostroha, M. Yukhymenko, J. Bocko, and J. Krmela, "Convective drying in the multistage shelf dryers: theoretical bases and practical implementation", in *Drying Unit Operations*, pp. 140–163, IntechOpen, UK, 2019.

[27] A.E. Artyukhov and V.I. Sklabinskiy, "Application of vortex three-phase separators for improving the reliability of pump and compressor stations of hydrocarbon processing plants", *IOP Conf. Ser.: Mater. Sci. Eng.* 233(1), 012014 (2017).

[28] K. Hiltunen, A. Jasberg, S. Kallio, H. Karema, M. Kataja, A. Koponen, M. Manninen, and V. Taivassalo, *Multiphase Flow Dynamics: Theory and Numerics*, VTT Technical Research Centre of Finland, Edita Prima Oy, 2009.

[29] C. Crowe, *Multiphase flow handbook*, Boca Raton, Taylor & Francis Group, 2006.

[30] D.L. Marchisio and R.O. Fox, *Computational Models for Polydisperse Particulate and Multiphase Systems*. Cambridge Series in Chemical Engineering. Cambridge University Press, 2013.

[31] D. Gidaspow, *Multiphase flow and fluidization: continuum and kinetic theory descriptions with applications*, Academic Press, San Diego, 1994.

[32] E.G. Sinaiski, *Hydromechanics: theory and fundamentals*, Weinheim, WILEY-VCH Verlag GmbH & Co. KGaA, 2010.

[33] A.E. Artyukhov and N.O. Artyukhova, "Technology and the main technological equipment of the process to obtain NH_4NO_3 with nanoporous structure", *Springer Proc. Phys.* 221, 585–594 (2019).

[34] K.P. Bowman, J.C. Lin, A. Stohl, R. Draxler, P. Konopka, A. Andrews, and D. Brunner, "Input Data Requirements for Lagrangian Trajectory Models", *Bull. Am. Meteorol. Soc.* 94, 1051–1058 (2013).

[35] M. Rybalko, E. Loth, and D. Lankford, "A Lagrangian particle random walk model for hybrid RANS/LES turbulent flows", *Powder Technol.* 221, 105–113 (2012).

[36] A.I. Leont'ev, Yu. A. Kuzma-Kichta, and I. A. Popov, "Heat and mass transfer and hydrodynamics in swirling flows (review)", *Therm. Eng.* 64(2), 111–126 (2017).

[37] M. Honkanen, *Direct optical measurement of fluid dynamics and dispersed phase morphology in multiphase flows*, p. 193, PhD. Thesis, Tampere Univetsity of Technology, 2006.

[38] M.J.V. Goldschmidt, G.G.C. Weijers, R. Boerefijn, and J.A.M Kuipers, "Discrete element modelling of fluidised bed spray granulation", *Powder Technol.* 138, 39–45 (2003).

[39] M. Khanali, S. Rafiee, A. Jafari, and A. Banisharif, "Study of Residence Time Distribution of Rough Rice in a Plug Flow Fluid Bed Dryer", *Int. J. Adv. Sci. Technol.* 48, 103–114 (2012).

[40] S. Banerjee and R.K. Agarwal, "Review of recent advances in process modeling and computational fluid dynamics simulation of chemical-looping combustion", *Int. J. Energy Clean Environ.* 18(1), 1–37 (2018).

[41] Certificate of copyright registration No. 79141UA, UA: Computer program "Multistage fluidizer", 2018.

[42] B. Paprocki, A. Pregowska and J. Szczepanski, "Optimizing information processing in brain-inspired neural networks", *Bull. Pol. Acad. Sci. Tech. Sci.* 68(2), 225–233 (2020), doi: 10.24425/bpasts.2020.131844.

[43] W. Jefimowski, A. Nikitenko, Z. Drążek, and M. Wieczorek, "Stationary supercapacitor energy storage operation algorithm based on neural network learning system", *Bull. Pol. Acad. Sci. Tech. Sci.* 68(4), 733–738 (2020), doi: 10.24425/bpasts.2020.134176.